Interface model for fracture behaviour of Fiber-Reinforced Cementitious Composites (FRCCs): theoretical formulation and applications

Antonio Caggiano* — **Guillermo Etse**** — **Enzo Martinelli***

* *Department of Civil Engineering (DiCiv - UniSA), Via Ponte don Melillo, University of Salerno, 84084, Fisciano (SA), Italy.*

ancaggiano@unisa.it (A.Caggiano), e.martinelli@unisa.it (E.Martinelli).

** *CONICET, Center for Numerical and Computational Methods in Engineering (CEMNCI), Universidad Nacional de Tucumán, Avda. Independencia 1800, 4000, San Miguel de Tucumán, Argentina.*

getse@herrera.unt.edu.ar (G.Etse).

ABSTRACT. *This paper presents a model for fiber-reinforced cementitious composites (FRCCs) based on a cohesive-frictional interface theory. A zero-thickness joint model is formulated for simulating the fracture behaviour of interfaces between the various phases of fiber-reinforced concretes. In particular, the "Mixture Theory" is used for describing the coupled action between concrete and fibers. Numerical analyses have been carried out on both plain concrete and FRCC members. Comparisons between numerical simulation and experimental evidence demonstrate the accuracy and soundness of the proposed formulation.*

RÉSUMÉ. *Cet article présentes une théorie pour simuler la réponse non linéaire des matériaux composites en béton fibré (FRCC). Une modèle d'interface sans épaisseur a été formulé pour simuler le comportement à la fracture entre les plusieurs phases du béton fibré. En particulier, la "Théorie des Mixtures" a été utilisé pour reproduire l'action couplée de béton et fibres. Enfin, la comparaison entre des résultats numériques et les correspondents donnés expérimentales montres le potentiel du modèle proposé.*

KEYWORDS: *Fiber-reinforced concrete; Fiber Bond; Mixture Theory; Constitutive laws.*

MOTS-CLÉS : *Béton fibré; Adhérence des fibres; Théorie des Mixtures; Lois constitutives.*

1. Introduction

The mechanical behaviour of concrete-based materials is greatly affected by crack propagation under general stress states. The presence of one or more dominant cracks in structural members modifies the material behaviour, possibly leading to brittle failure modes. The random dispersion of short steel fibers in cement materials is a new methodology used for enhancing the response in the post-cracking regime. The behaviour of fiber-reinforced cementitious composite (FRCC) compared to conventional plain concrete, is characterised by several advantages, e.g., higher tensile and shear resistance, better post-cracking ductility, higher fracture energy, etc.

Theoretical models and numerical procedures are needed for describing both cracking onset and propagation in non-homogeneous quasi-brittle materials such as FRCC (di Prisco *et al.*, 2009). In fact, simulating cracking phenomena in solids is still an open issue in computational mechanics. In current practice of finite element analyses, cracking in concrete structures is predominantly modelled through smeared crack approaches as proposed by Rots *et al.* (1985), Oliver (1989) and others. The finite element size dependence (mesh-bias) in softening responses is the main drawback of those classes of models (Bazant *et al.*, 1983).

The definition of possible discontinuities within the displacement field is needed for overcoming the above mentioned drawback of general FEM models. Several models and techniques have been proposed in the scientific literature and are outlined in the following paragraphs.

Strong discontinuity approaches: they allow for displacement discontinuities into the finite element formulations for capturing all arbitrary crack propagations with a fixed FE mesh without loss of mesh objectivity. The embedded strong discontinuity finite elements (E-FEM) proposed among others by Dvorkin *et al.* (1990) and Oliver (1996), and the extended finite element method (X-FEM) in Wells *et al.* (2001) are modern FE techniques employing this class of approaches. An interesting and innovative proposal to model strong discontinuities in concrete materials has been proposed by Oliver *et al.* (2004).

Lattice models: within the framework of meso-mechanical studies for fracture behaviour of concrete elements, the lattice models are simple and effective tools for understanding the physics of fracture processes. Lattice type models can be based on either truss elements (Schorn *et al.*, 1987) or beam ones (Lilliu *et al.*, 2003).

Particle models: these models are based on the formulation of the microscopic inter-particle contact layers of the matrix particles. Among various proposals, a particle model for brittle aggregate composite materials has been proposed by Bazant *et al.* (1990), for simulating cracking localisation in concrete elements.

Element-free Galerkin: this method represents an another attractive tool for modelling the propagation of material cracks. Significant contributions are given in (Belytschko *et al.*, 1995) and (Zhang *et al.*, 2008).

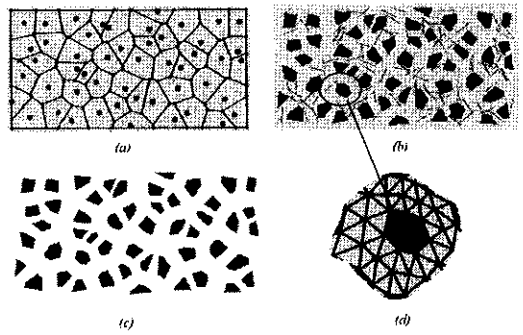

Figure 1. *2D meso-structure geometry: (a) Delaunay triangulation/Voronoi tessellation (Idiart, 2009), (b) FRCC meso-probe, (c) coarse aggregates and (d) position of the interface elements.*

Zero-thickness interface models: an alternative approach for discrete finite element failure analysis is represented by interface crack models. Zero-thickness joints connect continuum solid elements throughout potential crack lines. The material failure in crack processes is captured by means of those elements for discrete constitutive analyses, relating contact stresses (in normal and/or tangential direction) and the relative displacements (crack opening and sliding) with specific constitutive models, e.g., Hillerborg *et al.* (1976), Carol *et al.* (1997), Pandolfi *et al.* (2002), Lorefice *et al.* (2008), etc.

This work presents an interface constitutive model for mesoscopic fracture analysis (Lopez *et al.*, 2008) of FRCCs. For this purpose, FRCC can be regarded as a four-phase material (figure 1), composed by (*i*) coarse aggregates, (*ii*) plain mortar, (*iii*) plain interfaces modelling the cementitious matrix-to-coarse aggregate interaction and (*iv*) FRCC interfaces for the matrix-to-matrix crack modelling.

The non-linear behaviour of steel fiber reinforced concrete/mortar is fully captured by means of the model formulation for zero-thickness joint elements (Caggiano *et al.*, 2011a). The constitutive proposal has been based on the original idea of Carol *et al.* (1997) modified and extended to fiber concrete composites on the basis of the well-known "Mixture Theory" (Truesdell *et al.*, 1960) also employed by Manzoli *et al.* (2008) for RC members.

Section 2 briefly repeats the interface model for FRCC. The softening behaviour of the interface model due to crack propagation has been modelled as outlined in section 3 by means of an incremental approach, which is similar to the one usually adopted in the classical flow theory of plasticity. A novel bond-slip model is presented in section 4, in order to simulate correctly the axial effect of fibers. The composite action between concrete and fiber reinforcements is also completed by considering the dowel fiber effect by means of the model given in 5. Finally, numerical simulations of available experimental test data are presented in section 6 to show the soundness and capabilities of the proposed methodology.

The meso-mechanical approach (and the consequent possibility of modelling the behaviour of FRCC starting from both their components and the interactions among them) is the key novelty of the proposed model. Thus, this paper is aimed at validating the proposed model which could be employed in further studies for simulating the sensitivity of the mechanical response of FRCCs to the various relevant geometric and mechanical parameters.

As a matter of principle, the huge aleatoric nature of FRCC (mainly deriving by the randomness in fiber orientation and distribution, aggregate size and collocation, mixing and casting procedures and so on, so forth) is the key reason why simulating the global behaviour of FRCCs starting from their constituents can lead to unreliable predictions of the global response of the composite material as a whole. Nevertheless, the basic interactions among the various components which actually affect the global response of FRCC can be modelled mechanically as proposed in the present paper and the natural randomness of the component properties and distribution can be handled within the framework of well established statistical procedures whose application is beyond the scopes of the present formulation.

2. General aspects of an interface model for FRCC

The relationship between stresses and relative displacements developed throughout the generic fracture, can be formulated in the following incremental form, as usual in plasticity-based model

$$\dot{\mathbf{t}} = \underline{\mathbf{E}}^{ep} \cdot \dot{\mathbf{u}} \qquad [1]$$

being $\dot{\mathbf{t}}$ the rate vector of the composite joint stresses and $\dot{\mathbf{u}}$ the interface displacement rate vector, respectively.

According to the basis of the "Mixture Theory", the composite contact is considered through an interface in which each infinitesimal surface is ideally and simultaneously occupied by all components. Each component is subjected to the same displacement field while the corresponding composite stress is given by the weighted sum of

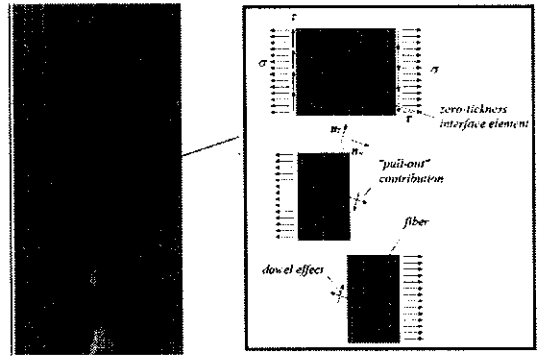

Figure 2. *Fiber effects on the plane of the zero-thickness interface.*

the stresses on each component. For the same assumption the constitutive tangent operator, $\mathbf{E}^{ep}$, is given by the following expression

$$\mathbf{E}^{ep} = w[\rho_i]\mathbf{C}^{ep} + \sum_{f=1}^{n_f} w[\rho_f]\left(\frac{E_f^{ep}}{l_f}\mathbf{n_N} \otimes \mathbf{n_N} + \frac{G_f^{ep}}{l_f}\mathbf{n_T} \otimes \mathbf{n_T}\right) \qquad [2]$$

based on the weighting functions $w[\rho_\#]$ (# = i, f, where the scripts i and f refer to interface and fiber, respectively) defined in Caggiano *et al.* (2011a), $\rho_\#$ represents the volume fraction of the # composite component, $\mathbf{n_N}$ and $\mathbf{n_T}$ are two unit vectors identifying the direction and its orthogonal, respectively, of a generic fiber with respect to the global Cartesian reference system, l_f and n_f represent the length measure and the number of the considered fibers.

The tangent operators $\left\{\mathbf{C}^{ep}, E_f^{ep}, G_f^{ep}\right\}$ of equation [2] have been defined as follows:

fracture-based plain interface model:

$$\mathbf{C}^{ep} = \partial \mathbf{t}^i / \partial \mathbf{u}. \qquad [3]$$

formulated in terms of normal (σ_N) and shear (σ_T) stresses ($\mathbf{t}^i = [\sigma_N, \sigma_T]^t$) of plain concrete joints corresponding to the relative displacements $\mathbf{u}$ (further details have been briefly explained in section 3);

bond-slip fiber-to-concrete model:

$$E_f^{ep} = d\sigma_f / d\varepsilon_N, \qquad [4]$$

being σ_f and ε_N the axial stress and strain of fibers at cracks (ideally assuming that each fiber crosses the interface fracture surface at mid-length, i.e. $l_f/2$); a closed-form analytical constitutive model ($\sigma_f - \varepsilon_N$ law) for the debonding fiber process is considered by enhancing a previous model by Caggiano *et al.* (2011b) (see section 4 for further details);

dowel action model:

$$G_f^{ep} = d\tau_f / d\delta_T, \qquad [5]$$

in which the elastic branch of the shear stress-strain law ($\tau_f - \gamma_T$) is derived by modelling the fiber embedded into the cement matrix as a Winkler foundation beam (as presented in section 5).

Fiber bridging effects, formulated herein in terms of bond-slip and dowel mechanisms, are schematically represented as in figure 2. The number of fibers per interface, radially distributed in the crack plane with the same angle spacing, is explicitly been considered in the present paper. For instance, a theoretical expression for evaluating the number of short reinforcements per unit cross-sectional area by Soroushian *et al.* (1990).

3. Interface constitutive model for plain concrete/mortar

In this section a rate-independent fracture-based plasticity model is considered. The main aspects of the interface model have been detailed in Caggiano *et al.* (2011a) and briefly presented in table 1, where C defines the uncoupled normal/tangential elastic stiffness matrix, $\dot{\mathbf{u}}^{ei}$ and $\dot{\mathbf{u}}^{cr}$ the vector of the elastic and cracking displacement rate (this latter according to the non-associated flow rule), respectively, $f(\mathbf{t}^i, \kappa)$ is a hyperbola (Carol *et al.*, 1997) defining the yield condition of the model on the bases of the three-parameters: χ (tensile strength), c (cohesion) and ϕ (friction angle).

The cracking displacement rate, $\dot{\mathbf{u}}^{cr} = [\dot{u}^{cr}, \dot{v}^{cr}]^t$ ($\dot{u}^{cr}$ and $\dot{v}^{cr}$ represent the normal and the tangential components, respectively, while t interprets the transposition vector operator), is given with a general non-associated flow rule which controls the direction, $\mathbf{m}$, of the interface fracture displacements by means of the transformation matrix operator $\mathbf{A}$ applied to the associated normal flow direction, $\mathbf{n}$, $\dot{\lambda}$ is the non-negative plastic multiplier derived by means of the Kuhn-Tucker loading/unloading conditions.

Table 1 defines the incremental fracture work, $\dot{w}_{cr}$, which controls the evolution of the yielding surface in a generic fracture process. A unified decay function, similar to the one proposed by Carol *et al.* (1997) is considered for each internal parameter, p_i (alternatively equals to χ, c or $\tan\phi$), of the yield condition: p_{i_0} is the initial value, $_{1p}p_{i_0}$ the residual one and $S[\xi_{p_i}]$ the scaling function, with ξ_{p_i} which measures the ratio between the current work spent in fracture and the available fracture energy.

	Fracture - based energy interface model
Constitutive equation	$\dot{\mathbf{t}} = \mathbf{C} \cdot (\dot{\mathbf{u}} - \dot{\mathbf{u}}^{cr})$ $\dot{\mathbf{u}} = \dot{\mathbf{u}}^{el} + \dot{\mathbf{u}}^{cr}$
Yield condition	$f(\mathbf{t}^r, \kappa) = \sigma_T^2 - (c - \sigma_N \tan\phi)^2 + (c - \chi \tan\phi)^2$
Flow rule	$\dot{\mathbf{u}}^{cr} = \dot{\lambda}\mathbf{m}$ $\mathbf{m} = \mathbf{A} \cdot \mathbf{n}$
Cracking work evolution	$\dot{\kappa} = \dot{w}_{cr}$ $\dot{w}_{cr} = \sigma_N \cdot \dot{u}^{cr} + \sigma_T \cdot \dot{u}^{cr}$ if $\sigma_N \geq 0$ $\dot{w}_{cr} = \lvert\sigma_T - \lvert\sigma_N\rvert \tan(\phi)\rvert \cdot \dot{u}^{cr}$ if $\sigma_N < 0$
Evolution law	$p_i = [1 - (1 - r_p) S_{ii}^2] p_{i0}$
Kuhn - Tucker loading/unloading	$\dot{\lambda} \geq 0, \quad f(\mathbf{t}^r, \kappa) \leq 0, \quad \dot{\lambda} f(\mathbf{t}^r, \kappa) = 0$

Table 1. *Overview of the interface model for Plain Concrete/Mortar.*

4. Closed-form pull-out analysis of a single fiber

Figure 3 shows an isolated fiber loaded by a pulling force, P_i. The fiber is embedded in a cementitious matrix for a l_{emb} length measure. The equilibrium scheme given in the figure is used to simulate the complete slipping behaviour. The following basic equations have been used for analysing the fiber-to-concrete debonding process:

Equilibrium: $\frac{d\sigma_f(x)}{dx} = -\frac{4\tau_a(x)}{d_f}$, being σ_f the axial stress of the fiber, τ_a the shear bond stress and d_f the diameter of the fiber.

Fiber constitutive law in axial direction: $\sigma_f(x) = E_s \frac{ds(x)}{dx}$, with E_s the elastic steel modulus and $s(x)$ the slip between fiber and surrounding concrete mortar based on the assumption of figure 3.

Bond constitutive law: $\tau_a(x) = \begin{cases} -k_E s(x) & s(x) \leq s_e \\ -\tau_{y,a} + k_S (s(x) - s_e) & s_e < s(x) \leq s_u \\ 0 & s(x) > s_u \end{cases}$,

where, assuming a bilinear $\tau_a - s$ law, k_E and $-k_S$ represents the slope of the elastic and softening branches of the bond-slip relationship, respectively, $\tau_{y,a}$ whereas is the maximum shear stress. Thus, $s_e = \frac{\tau_{y,a}}{k_E}$ and s_u represent the elastic and the ultimate slips, respectively.

As schematically reported in table 4 and based on the approach proposed by Yuan *et al.* (2004) for FRP laminates under pull-out, different states of the bond response have been defined. The fiber-to-concrete interface is in elastic bond state (E) if $s(x) \leq s_e$, in softening state (S) when $s_e < s(x) \leq s_u$, or the bond is crushed if $s(x) > s_u$. A combination of three stress states can occur throughout the bonding length during the pull-out process of the single fiber (see table 4). Fully elastic behaviour of fibers has been assumed. This is strictly true in the case of synthetic fibers,

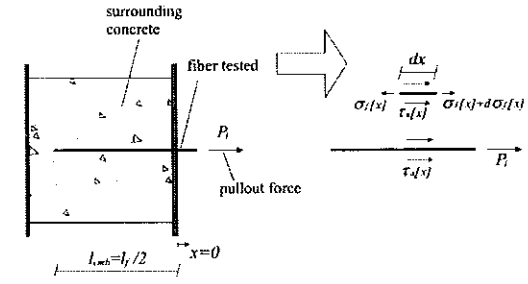

Figure 3. *Pull-out of a single fiber reinforcement.*

Slips	Type of joint adherence
$s(x) \leq s_e \forall x \in [-l_{emb}, 0]$	Elastic Response (E)
$s(x) \leq s_e \forall x \in [l_{emb}, l_e]$ $s_e < s(x) \leq s_u \forall x \in [-l_e, 0]$	Elastic – Softening Response (ES)
$s_e < s(x) \leq s_u \forall x \in [-l_{emb}, 0]$	Softening Response (S)
$s(x) \leq s_e \forall x \in [l_e, -l_e]$ $s_e < s(x) \leq s_u \forall x \in [l_e, -l_u]$ $s(x) > s_u \forall x \in [-l_u, 0]$	Elastic – Softening – Debonding (ESD)
$s_e < s(x) \leq s_u \forall x \in [-l_{emb}, -l_u]$ $s(x) > s_u \forall x \in [-l_u, 0]$	Softening – Debonding Response (SD)
$s(x) > s_u \forall x \in [-l_{emb}, 0]$	Debonding Failure (D)

being $-l_e$ ($0 \leq l_e \leq l_{emb}$) and $-l_u$ ($0 \leq l_u \leq l_{emb}$) the abscissas of the points in which the local slip is equal to the elastic limit (s_e) and the ultimate value (s_u), respectively.

Table 2. *Bond response of the fiber-concrete joint depending on the slip $s(x)$ developed throughout the embedment length.*

while can be accepted for steel ones when the length l_{emb} results in the condition of $P_{i,max} < \sigma_{y,s} A_f$, where $\sigma_{y,s}$ is the fiber yielding stress and A_f the area of transverse section.

For the sake of simplicity, the description of the complete analytical pull-out model will be given in a future work completely dedicated to the pull-out modelling.

4.1. *1D elasto-plastic model*

The uniaxial behaviour of the steel fiber to account in the composite model of section 2 is approached through a simple 1D elasto-plastic model. The incremental stress-strain relationship, can be written as

$$\dot{\sigma}_f = E_f^{ep} \dot{\varepsilon}_N \qquad [6]$$

where the elasto-plastic tangent module E_f^{ep} takes the two distinct following values (Simo *et al.*, 1998)

$$\begin{cases} E_f^{ep} = E_f & \rightarrow \text{elastic/unloading response} \\ E_f^{ep} = \frac{E_f H_f}{E_f - H_f} & \rightarrow \text{elasto-plastic regime} \end{cases} \qquad [7]$$

in which E_f is the initial stiffness of the bond-slip model and H_f the hardening/softening modulus.

The model is based on the following yielding condition

$$f_f = |\sigma_f| - (\sigma_{y,f} + Q_f) \leq 0 \qquad [8]$$

being $\sigma_{y,f}$ the slipping bond strength and Q_f the internal softening variable in post-elastic regime.

The pull-out behaviour of a single fiber has been modelled through a closed-form relationship proposed by Caggiano *et al.* (2011b) for similar problem involving FRP plates glued on concrete surfaces.

4.2. *Verification of the pull-out model*

Some numerical examples are reported in this section to show the main features of the proposed bond-slip analytical model for SFRC model. The verification examples include pull-out tests of both straight and hooked fibers. Test data by Lim *et al.* (1987) regarding pull-out probes have been considered which relevant properties of fibers are listed as follows:

- *Straight fibers*: $d_f = 0.565\,mm$ (diameter), $\sigma_{y,s} = 345\,N/mm^2$ (strength), $E_s = 210\,GPa$ (elastic modulus).
- *Hooked fibers*: $d_f = 0.500\,mm$ (diameter), $\sigma_{y,s} = 1130\,N/mm^2$ (strength), $E_s = 200\,GPa$ (elastic modulus).

Figure 4 shows the $P_i - s_i$ curves (pull-out action vs. applied slip) for straight and hooked fibers with different embedment lengths based on the model parameters defined in table 3.

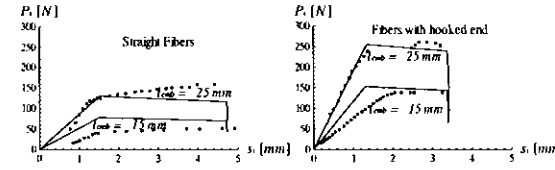

Figure 4. *Pull-out experiments (discontinuous lines) by Lim* et al. *(1987) on straight and hooked-end fibers vs. numerical results (continuous lines).*

	MaterialParameters			
	$\tau_{y,o}[MPa]$	$k_E[MPa/mm]$	$k_S[MPa/mm]$	$s_u[mm]$
StraightFibers	3.0	2.0	0.1	4.725
HookedFibers	6.0	5.0	0.2	3.380

Table 3. *Model parameters for pull-out tests by Lim* et al. *(1987).*

The proposed model leads to good predictions of the behaviour of both fiber types, capturing the increment of strength as the embedment measure increases. The presence of hooked ends in fibers determines an increase in shear strength, $\tau_{y,o}$, compared to straight fibers and a decrement of the ductility of the contact. In fact, the elastic and softening slopes (k_E and k_S, respectively) increase considering hooked fibers, while a decrease in the ultimate slip, s_u, passing from straight to hooked fibers can be observed.

5. Analytical model for fiber-to-concrete dowel action

The dowel action of steel fibers bridging concrete fractures is described by means of a 1-D elasto-plastic model, characterised by a simple linear softening law.

Within the framework of the flow plasticity theory, the complete model is described by means of the following set of equations:

- *Yield function*: $g_f = |\tau_f| - (\tau_{y,f} + Q_{dow}) \leq 0$, when τ_f is the dowel shear stress, $\tau_{y,f}$ the dowel strength and Q_{dow} the stress-like measure.
- *Softening law*: $\dot{Q}_{dow} = \dot{\lambda}_f H_{dow}$, where $\dot{\lambda}_f$ and H_{dow} are the plastic multiplier and the hardening/softening modulus, respectively.

Flow rule: $\dot{\gamma}_T^{pl} = \dot{\lambda}_f \partial g_f / \partial \tau_f = \dot{\lambda}_f sign[\tau_f]$, where $\dot{\gamma}_f^{pl}$ is the rate of the plastic dowel strain.

The constitutive law between the dowel shear stress, τ_f, and the corresponding equivalent shear strain, γ_T, can be written in incremental form as follows

$$\dot{\tau}_f = G_f^{TP} \dot{\gamma}_T \qquad [9]$$

being G_f^{TP} the tangent modulus expressed in terms of the initial dowel stiffness G_f and the hardening/softening modulus H_{dow}, depending on the loading or unloading/elastic situation

$$\begin{cases} G_f^{TP} = G_f & \rightarrow \text{unloading/elastic} \\ G_f^{TP} = \frac{G_f H_{dow}}{G_f + H_{dow}} & \rightarrow \text{loading} \end{cases} \qquad [10]$$

5.1. *Dowel stiffness*

The analytical model used to predict the dowel behaviour of fibers embedded in concrete composites has been based on the analysis of a beam on elastic foundation (BEF). The following differential equation for the deflection equilibrium of a BEF can written

$$\frac{d^4 \Delta(x)}{dx^4} + 4\lambda^4 \Delta(x) = 0 \qquad \text{with} \qquad \lambda^4 = \frac{k_c}{4E_s J_s} \qquad [11]$$

being $\Delta(x)$ the deflection of the beam, k_c the elastic stiffness of the spring foundation modelling the surrounding cementitious matrix, E_s and J_s are the elastic modulus of the steel and the inertia of the fiber, respectively, and finally λ represents a characteristic length of the Winkler beam.

Let us consider the case of fibers supposed to be "semi-infinite" BEF, the following equations govern the problem

$$\begin{array}{l} \Delta(x) = A_1 e^{-\lambda x}\cos(\lambda x) + A_2 e^{-\lambda x}\sin(\lambda x) \\ M_d(x) = 2E_s J_s \lambda^2 e^{-\lambda x}[A_2\cos(\lambda x) - A_1 \sin(\lambda x)] \\ V_d(x) = -2E_s J_s \lambda^3 e^{-\lambda x}[(A_2 - A_1)\sin(\lambda x) + (A_1 + A_2)\cos(\lambda x)] \end{array} \qquad [12]$$

being M_d and V_d the bending moment and the dowel action at $l_f/2$ of the steel fiber, while A_1 and A_2 are constants deriving by the boundary conditions.

The analytical solution of the semi-infinite BEF problem is based on the assumption that the crack width is considered null and supposing that in $x = 0$ the moment is null (inflection point). Then, considering an applied dowel force, V_d, at the loaded end ($x = 0$), the following analytical deflection is obtained

$$\Delta(x) = -\frac{e^{-\lambda x}\cos(\lambda x)}{2\lambda^3 E_s J_s} V_d \qquad [13]$$

Finally, the $V_d - \Delta_0$ law in correspondence of the considered crack ($x = 0$) takes the following expression

$$\begin{array}{l} V_d = \lambda^3 E_s J_s \Delta_0 \rightarrow \frac{V_d}{A_f} = \frac{l_f}{A_f}\lambda^3 E_s J_s \frac{\Delta_0}{l_f} \\ \qquad\qquad \Rightarrow G_f = \frac{l_f}{A_f}\lambda^3 E_s J_s \end{array} \qquad [14]$$

also expressed in terms of $\tau_f - \gamma_T \left\{ \frac{V_d}{A_f} - \frac{\Delta_0}{l_f} \right\}$ law, from which the dowel stiffness, G_f, can be derived. In equation [14] $A_f = \pi \frac{d_f^2}{4}$ is the cross section area of a single fiber.

The elastic foundation stiffness of the surrounding concrete, k_c, assumes the following empirical expression (Soroushian *et al.*, 1987)

$$k_c = \kappa_1 \frac{\sqrt{f_c'}}{{d_f}^{4/3}} \qquad [15]$$

being f_c' the compression strength of the surrounding cementitious matrix and κ_1 a coefficient to be calibrated.

5.2. *Dowel strength*

Typical failures in the fiber dowel are characterised by local crushing of the surrounding matrix and/or yielding of the steel fiber. For these reasons, the following empirical expression (Dulacska, 1972), considering both failure modes, is employed

$$V_{d,u} = k_{dow} d_f^2 \sqrt{\frac{1}{3} f_c' \frac{1}{3} \sigma_{y,s}} \qquad [16]$$

being k_{dow} a non-dimensional coefficient which typical value $k_{dow} = 1.2\tau$ could be assumed as a reference for RC-structures (Dulacska, 1972).

Finally, the equivalent dowel strength $\tau_{y,f}$ can be defined through the yielding criterion assumed for the dowel action

$$\tau_{y,f} = \frac{V_{d,u}}{A_f}. \qquad [17]$$

6. Applications

This section presents the key results obtained in several numerical analyses performed at both material and structural level of observation of the failure behaviour of tests made out of either plain or SFRC materials.

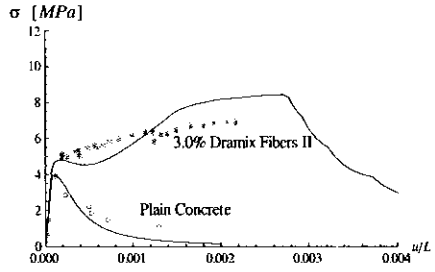

Figure 5. *Experimental results by Li* et al. *(2001) (discontinuous lines) and numerical predictions (continuous lines) for SFRC in tension with Dramix type II and* $\rho_f = 3.0\%$.

6.1. *SFRC under tensile loads*

The proposed constitutive model is used to predict the macroscopic tensile response in terms of average stress vs. nominal strain (namely u/L) for several experimental tests on SFRC specimens. The length L corresponds to the axial distance between the two LVDTs considered by Li *et al.* (2001) for determining axial strains from measured relative displacements, u. The comparisons between the model predictions and the experimental data by Li *et al.* (2001) are reported in figure 5 to 10. The considered SFRC specimens contain two fiber types, namely "Dramix type I" and "Dramix type II" whose fundamental characteristics are listed below:

- **Dramix type I**: steel fibers with diameter $d_f = 0.5\ mm$, fiber length $l_{f,1} = 30\ mm$, density $\gamma_f = 7.8\ g/cm^3$, tensile strength $f_{fu} = 1.20\ GPa$ and elastic modulus $E_f = 200\ GPa$.
- **Dramix type II**: steel fibers with diameter $d_f = 0.5\ mm$, fiber length $l_{f,2} = 50\ mm$, density $\gamma_f = 7.8\ g/cm^3$, tensile strength $f_{fu} = 1.20\ GPa$ and elastic modulus $E_f = 200\ GPa$.

Figures 5 to 7 depict the stress-strain response for SFRCs with steel Dramix type II whose fiber contents, ρ_f, are 3.0%, 3.5% and 4.0%, respectively. While figures 8 to 10 outline SFRC tests characterised by Dramix fiber type I with 6.0%, 7.0% and 8.0% of volume fiber content, respectively.

The calibrated parameters, based on a least-square procedure outlined in Caggiano *et al.* (2011a) and given in table 4, are referred on the experimental data of figure 8. All

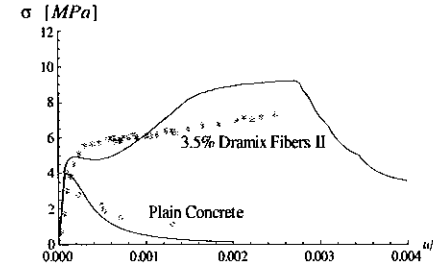

Figure 6. *Experimental results by Li* et al. *(2001) (discontinuous lines) and numerical predictions (continuous lines) for SFRC in tension with Dramix type II and* $\rho_f = 3.5\%$.

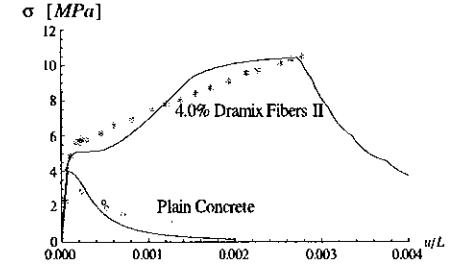

Figure 7. *Experimental results by Li* et al. *(2001) (discontinuous lines) and numerical predictions (continuous lines) for SFRC in tension with Dramix type II and* $\rho_f = 4.0\%$.

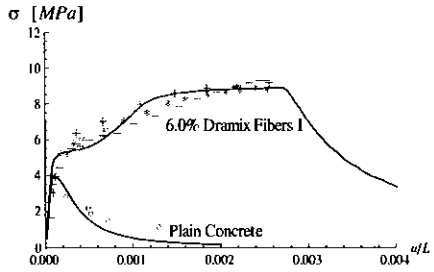

Figure 8. *Experimental results by Li* et al. *(2001) (discontinuous lines) and numerical predictions (continuous lines) for SFRC in tension with Dramix type I and* $\rho_f = 6.0\%$.

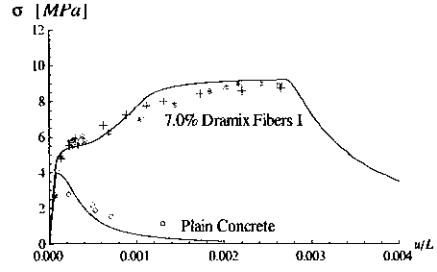

Figure 9. *Experimental results by Li* et al. *(2001) (discontinuous lines) and numerical predictions (continuous lines) for SFRC in tension with Dramix type I and* $\rho_f = 7.0\%$.

the other numerical curves have been obtained by just changing the fiber contents (n_f, number of fiber per interfaces) and/or fiber type (i.e., $l_f = l_{f,1}$ or $l_{f,2}$) according to the specimen properties. The possibility of modelling variation in the structural response at the global level by just modifying the geometrical data describing the amount of fibers is the key advantage of approaching the simulation of FRCCs at the meso-scale.

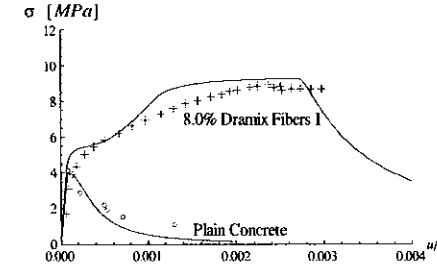

Figure 10. *Experimental results by Li* et al. *(2001) (discontinuous lines) and numerical predictions (continuous lines) for SFRC in tension with Dramix type I and* $\rho_f = 8.0\%$.

	SFRC Interface Material Parameters			
Plain Interface	$k_N\,[MPa/mm]$ $1\,E+03$	$k_T\,[MPa/mm]$ $2\,E+02$	$\chi_0\,[MPa]$ 4.0	
	$c_0\,[MPa]$ 7.0	$tg\varphi_0 = tg\varphi_r = tg\,\delta$ 0.6	$G_I^{fi}\,[N/mm]$ 0.12	
	$G_I^{fi}\,[N/mm]$ 1.20	$\sigma_{act}\,[MPa]$ 10.0	α_χ −0.15	
Bond – slip Model	$\tau_{s,0}\,[MPa]$ 2.35	$k_E\,[MPa/mm]$ 52.5	$k_S\,[MPa/mm]$ 1.7	$s_2\,[mm]$ 0.137
Dowel Strength	κ_1 6.5	f_c' $10\cdot\chi_0$	k_{dowel} 0.23	

Table 4. *SFRC material parameters modelling the experimental data by Li* et al. *(2001).*

The numerical predictions compared against the experimental data (figure 5 to 10) show a very good agreement and represent a rather promising result. It can be noted that only the hardening regime of the SFRC response have been reported by the experimental tests given in Li *et al.* (2001). However, the model predicts in a very realistic mode the mechanical response of "ductile SFRC" when exhibits a tensile strain-hardening behaviour (typically, characterised by a continuous formation of

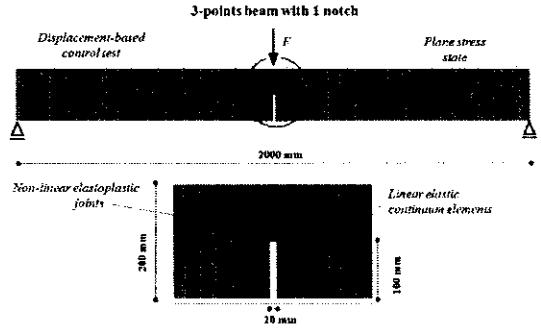

Figure 11. *Three-point bending test discretisation on a notched beam for discrete failure analyses.*

multiple cracks) which follows a localised crack mode at which the composite material begin to fail in a softening-brittle manner.

The presented tests demonstrate that a lower fiber content can be mechanically replaced by an increment of the fiber length. The post-cracking behaviour mainly depends on the fiber-to-concrete interactions in terms of fiber pull-out and dowel effect. Similar tensile strain-hardening responses, in post-cracking regime, can be obtained employing Dramix Fibers type II (which are $5/3$ longer than the type I fibers), considering a smaller content of steel reinforcements respect to the type I. The proposed model captures very well those aspects and demonstrates its capability of modelling composite steel fiber concrete structures.

6.2. *Notched beams under Tree-Point bending*

To assess the soundness of the proposed non-linear cracking model for interface elements, the results of tests on a notched beam under three-point bending are considered (figure 11). Several interface elements have been placed between adjacent isoparametric 3-node elements for modelling the fracture process of beams tested under the lay-out shown in figure 11.

Plane stress conditions, considering a depth of the beam $b = 50\,mm$ according to the experimental tests by Rots *et al.* (1985), are imposed in the numerical analyses at the mesoscopic level of observation. Plain concrete test is performed by imposing a

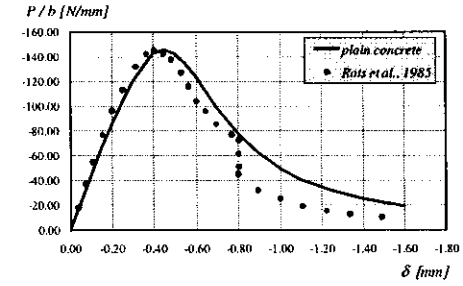

Figure 12. *Numerical results vs. experimental data by Rots* et al. *(1985) on a 3-point beam.*

homogeneous vertical displacement at mid-length of the considered beam. The results in terms of vertical applied deflection (δ) vs. vertical specific force (P/b) have been plotted in figure 12, where the numerical test is compared against the experimental measures performed by Rots *et al.* (1985).

The proposed interface model for mesoscopic analyses of concrete members leads to accurate simulations of both the peak strength and post-peak behaviour. A realistic deformed configuration at failure is also plotted in figure 13 where the mesh results in terms of vertical displacements and in terms of the w_{cr}/G_f^I ratio on the developed crack is plotted. Table 5 outlines the values of the key parameters related to the analysis of the three-point flexural test presented in this section. The remaining parameters have been set to zero in the proposed simulation.

7. Conclusions

The present paper proposes a novel model for simulating the cracking behaviour of fiber-reinforced cementitious composites (FRCCs). It can be employed on mesomechanical discontinuous analyses which concentrate all non-linearities of the structural response in zero-thickness interface elements connecting either aggregate to cement matrix or cement matrix to cement matrix. The formulation of the interface element for connecting nodes of two adjacent cement matrix elements is one of the key contribution of the present paper. It has been obtained by extending an interface model already available for analysing the behaviour of plain concrete members. Thus, the contribution of fibers bridging cracks possibly developing throughout those

Material Parameters			
Interface Elements	$k_N\,[MPa/mm]$	$k_T\,[MPa/mm]$	$\chi_0[MPa]$
	$1.E+06$	$1.E+06$	3.3
	$c_0[MPa]$	$tg\phi_0 = tg\phi_r = tg\beta$	$G_f^I[N/mm]$
	5.0	0.5	0.124
	$G_f^{II}[N/mm]$	$\sigma_{sa}[MPa]$	α_c
	1.240	3.6	-0.15
Continuum Elements	$E_m\,[MPa]$ (elastic module)		ν (Poisson's ratio)
	30000.0		0.2

Table 5. *Material parameters based on the experimental data by Rots* et al. *(1985).*

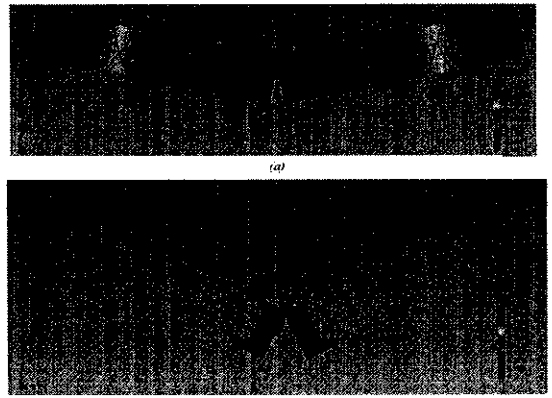

(a)

(b)

Figure 13. *Failure configuration in terms of (a) vertical displacement mesh informations and (b) work spent to available energy ratio of w_r/G_f^I.*

interfaces is modelled within the zero-thickness elements, along with the bonding behaviour of cement matrix.

Finally, applications of the numerical procedure to both notched plain concrete specimens tested under three-point-bending and FRCC samples in tension demonstrate the soundness of the proposed model and its accuracy in simulating the cracking behaviour of fiber-reinforced concrete members. The model simulates rather well several key features of the structural response of FRCCs (i.e., the tensile strain hardening behaviour of samples with enough fiber amount) and the natural randomness of the component properties and distribution could be handled within the framework of well established statistical procedures which can be possible employed in further developments of this research.

8. References

Bazant Z., Oh B., " Crack band theory for fracture of concrete", *Mater. Structures, RILEM*, vol. 93, p. 155-177, 1983.

Bazant Z., Tabbara M., Kazemi M., Pijaudier-Cabot G., " Random Particle Model for Fracture of Aggregate or Fiber Composites", *ASCE Journal of Engineering Mechanics*, vol. 116, n° 8, p. 1686-1705, 1990.

Belytschko T., Lu Y., Gu L., " Crack propagation by element-free Galerkin methods", *Engineering Fracture Mechanics*, vol. 51, n° 2, p. 295 - 315, 1995.

Caggiano A., Etse G., Martinelli E., " Zero-thickness interface model formulation for failure behavior of fiber-reinforced cementitious composites - Paper Submitted", *Computers & Structures*, 2011a.

Caggiano A., Martinelli E., Faella C., " A fully-analytical approach for modelling the response of FRP strips bonded to a stiff substrate - Paper Submitted", *Int. Journal of Solids and Structures*, 2011b.

Carol I., Prat P., Lopez C., " Normal/shear cracking model: Applications to discrete crack analysis", *ASCE - Journal of Engineering Mechanics*, vol. 123, p. 765-773, 1997.

di Prisco M., Plizzari G., Vandewalle L., " Fibre reinforced concrete: new design perspectives", *Materials and Structures*, vol. 42, p. 1261-1281, 2009.

Dulaeska H., " Dowel action of reinforcement crossing cracks in concrete", *ACI - Structural Journal*, vol. 69, n° 12, p. 754-757, 1972.

Dvorkin E., Cuitino A., Gioia G., " Finite elements with displacement embedded localization lines insensitive to mesh size and distortions", *International Journal for Numerical Methods in Engineering*, vol. 30, p. 541-564, 1990.

Han W., Reddy B., *Plasticity: Mathematical Theory and Numerical Analysis*, Springer, New York , 1999.

Hillerborg A., Modeer M., Petersson P., " Analysis of crack formation and crack growth in concrete by means of fracture mechanics and finite elements", *Cement and Concrete Research*, vol. 6, n° 6, p. 773-781, 1976.

Idiart A., Coupled analysis of degradation processes in concrete specimens at the meso-level, PhD thesis, Universitat Politecnica de Catalunya, ETSECCCP-UPC, 2009.

Kang H., Willam K., " Localization Characteristics of Triaxial Concrete Model", *ASCE - Journal of Engineering Mechanics*, vol. 125, n° 8, p. 941-950, 1999.

Li F., Li Z., " Continuum damage mechanics based modeling of fiber reinforced concrete in tension", *Int. Journal of Solids and Structures*, vol. 38, n° 5, p. 777-793, 2001.

Lilliu G., van Mier J., " 3D lattice type fracture model for concrete", *Engineering Fracture Mechanics*, vol. 70, p. 927-941, 2003.

Lim T., Paramasivam P., Lee S., " An analytical model for tensile behaviour of steel fiber concrete", *ACI - Materials Journal*, vol. 84, n° 4, p. 286-298, 1987.

Lopez C. M., Carol I., Aguado A., " Meso-structural study of concrete fracture using interface elements. I: numerical model and tensile behavior", *Materials and Structures*, vol. 41, n° 3, p. 583-599, 2008.

Lorefice R., Etse G., Carol I., " Viscoplastic approach for rate-dependent failure analysis of concrete joints and interfaces", *Int. Journal of Solids and Structures*, vol. 45, n° 9, p. 2686-2705, 2008.

Manzoli O., Oliver J., Diaz G., Huespe A., " Three-dimensional analysis of reinforced concrete members via embedded discontinuity finite elements", *Ibracon Structures and Materials Journal*, vol. 1, n° 1, p. 58-83, 2008.

Oliver J., " Consistent characteristic length for smeared cracking models", *International Journal for Numerical Methods in Engineering*, vol. 28, p. 461-474, 1989.

Oliver J., " Modelling strong discontinuities in solid mechanics via strain softening constitutive equation. 1. Fundamentals", *International Journal for Numerical Methods in Engineering*, vol. 39, p. 3575-3600, 1996.

Oliver J., Huespe A., Pulido M., Blanco S., " Computational modeling of cracking of concrete in strong discontinuity settings", *Computers and Concrete*, vol. 1, n° 1, p. 61-76, 2004.

Pandolfi A., Ortiz M., " An efficient adaptive procedure for three-dimensional fragmentation Simulations", *Engineering Computations*, vol. 18, p. 148-159, 2002.

Rots J., Nauta P., Kusters G., Blaauwendraad J., " Smeared crack approach and fracture localization in concrete", *Heron*, vol. 30, p. 1-49, 1985.

Schorn H., Rode U., *3-D modelling of process zone in concrete by numerical simulation*. In: Shah SP, Swartz SE, editors. Fracture of concrete and rock. New York: Springer Verlag; pp. 220-228, 1987.

Simo J., Hughes T., *Computational Inelasticity*, vol. 7, Interdisciplinary Applied Mathematics, Springer, New York, 1998.

Soroushian P., Lee C., " Distribution and orientation of fibers in steel fiber reinforced concrete", *ACI - Materials Journal*, vol. 87, n° 5, p. 433-439, 1990.

Soroushian P., Obaseki K., Rojas M., " Bearing strength and stiffness of concrete under reinforcing bars", *ACI - Materials Journal*, vol. 84, n° 3, p. 179-184, 1987.

Truesdell C., Toupin R., *The classical field theories*,, vol. III/1, Handbuch der Physik, Springer-Verlag, Berlin, 1960.

Wells G., Sluys L., " A new method for modelling cohesive cracks using finite elements", *International Journal for Numerical Methods in Engineering*, vol. 50, p. 2667-2682, 2001.

Yuan H., Teng J., Seracino R., Wu Z., Yao J., " Full-range behaviour of FRP-to-concrete bonded joints", *Engineering Structures*, vol. 26, n° 5, p. 553-565, 2004.

Zhang Z., Liew K., Cheng Y., Lee Y., " Analyzing 2D fracture problems with the improved element-free Galerkin method", *Engineering Analysis with Boundary Elements*, vol. 32, n° 3, p. 241 - 250, 2008.

ANNEXE POUR LE SERVICE FABRICATION
A FOURNIR PAR LES AUTEURS AVEC UN EXEMPLAIRE PAPIER
DE LEUR ARTICLE ET LE COPYRIGHT SIGNE PAR COURRIER
LE FICHIER PDF CORRESPONDANT SERA ENVOYE PAR E-MAIL

1. ARTICLE POUR LA REVUE :
L'objet. Volume 8 – n°2/2005

2. AUTEURS :
Antonio Caggiano[*] *— Guillermo Etse*[**] *— Enzo Martinelli*[*]

3. TITRE DE L'ARTICLE :
Interface model for fracture behaviour of Fiber-Reinforced Cementitious Composites (FRCCs): theoretical formulation and applications

4. TITRE ABREGÉ POUR LE HAUT DE PAGE MOINS DE 40 SIGNES :
Interface Fracture Model for FRCC

5. DATE DE CETTE VERSION :
September 23, 2011

6. COORDONNÉES DES AUTEURS :

– adresse postale :

[*] Department of Civil Engineering (DiCiv - UniSA), Via Ponte don Melillo, University of Salerno, 84084, Fisciano (SA), Italy.

ancaggiano@unisa.it (A.Caggiano), e.martinelli@unisa.it (E.Martinelli).

[**] CONICET, Center for Numerical and Computational Methods in Engineering (CEMNCI), Universidad Nacional de *Tucumán*, Avda. Independencia 1800, 4000, San Miguel de *Tucumán*, Argentina.

getse@herrera.unt.edu.ar (G.Etse).

– téléphone : 00 00 00 00 00

– télécopie : 00 00 00 00 00

– e-mail : guillaume.laurent@ens2m.fr

7. LOGICIEL UTILISÉ POUR LA PRÉPARATION DE CET ARTICLE :
LaTeX, avec le fichier de style `article-hermes.cls`,
version 1.23 du 17/11/2005.

8. FORMULAIRE DE COPYRIGHT :
Retourner le formulaire de copyright signé par les auteurs, téléchargé sur :
`http://www.revuesonline.com`

SERVICE ÉDITORIAL – HERMES-LAVOISIER
14 rue de Provigny, F-94236 Cachan cedex
Tél. : 01-47-40-67-67
E-mail : revues@lavoisier.fr
Serveur web : http://www.revuesonline.com